

Supplementary Figures

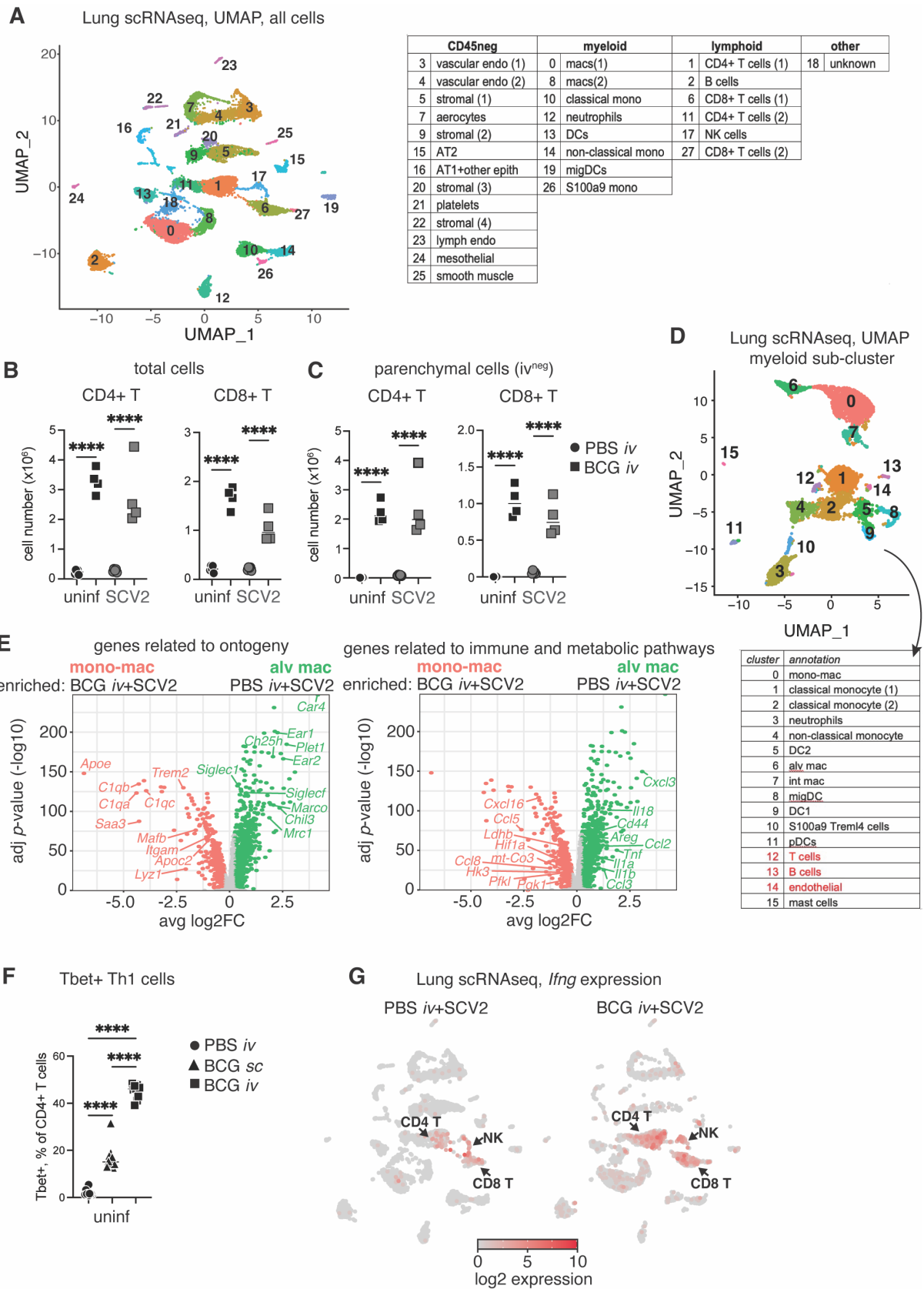


Figure S1: Th1 cells are enriched in the lung tissue following *iv* BCG.

B6 mice were inoculated with BCG *sc* or *iv* 40-45 days prior to intranasal challenge with SARS-CoV-2. Lungs were harvested 3 days after viral challenge. Control mice were not challenged with SARS-CoV-2 (uninf). **(A)** UMAP representation of scRNAseq data of whole lung isolated from BCG and PBS animals challenged with SARS-CoV-2 B.1.351. Clustering resolution: 0.6. Cell clusters were manually annotated and divided into 3 groups consisting of CD45-negative, myeloid or lymphoid lineages (table on right). Cluster specific gene sets are in Supplementary Data 1. Total number of lung CD4+ T cells and CD8+ T cells **(B)** and number of CD4+ T cells and CD8+ T cells located in the lung parenchyma (panCD45 *iv* negative) **(C)** as determined by flow cytometry. PBS $n=5$ /group, BCG $n=4$ /group; representative of 3 independent experiments; One-Way ANOVA with Tukey post-test. **** $p<0.0001$. **(D)** UMAP representation of re-clustered myeloid cells for PBS or BCG treated animals. Clustering resolution: 0.4. Cell clusters were manually annotated (table below). Cluster specific gene sets are in Supplementary Data 3. **(E)** Volcano plot shows DEGs between resident AM and monocyte-derived macrophage clusters with annotated cell ontogeny genes (left panel) and genes related to immune and metabolic pathways (right panel) ($\log_2FC>0.25$, $p<0.05$, Wilcoxon Rank Sum test with Bonferroni correction). Full gene lists and their associated FC and p -values are in Supplementary Data 4. **(F)** Frequency of lung Tbet+ CD4+ T cells as determined by flow cytometry (PBS $n=10$, BCG *sc* $n=10$, BCG *iv* $n=9$; pooled from 2 independent experiments; One-Way ANOVA with Tukey post-test). **** $p<0.0001$. **(G)** *Ifng* transcript expression overlaid on the UMAP from FigS1A separated by experimental condition. Source data are provided as a Source Data file.

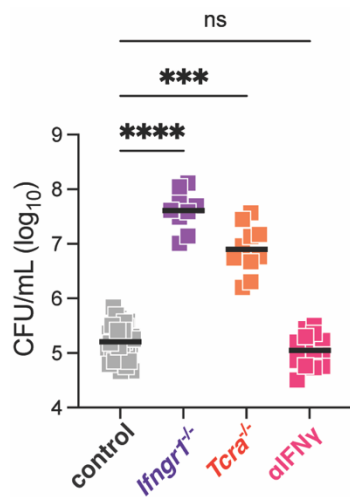


Figure S2: BCG CFU is not impacted by short-term IFN γ neutralization.

Mice of the indicated genotypes were inoculated with BCG *iv* 40-45 days prior to intranasal challenge with SARS-CoV-2. Lungs were harvested 3 days after viral challenge and plated on 7H11 agar to enumerate BCG CFU (B6 control $n=34$, *Ifngr1*^{-/-} $n=10$, *Tcra*^{-/-} $n=10$, α IFN γ $n=14$; pooled from 2-3 independent experimental Kruskal-Wallis with Dunn's post-test). Not significant (ns) $p>0.05$; *** $p=0.0003$; **** $p<0.0001$. Source data are provided as a Source Data file.

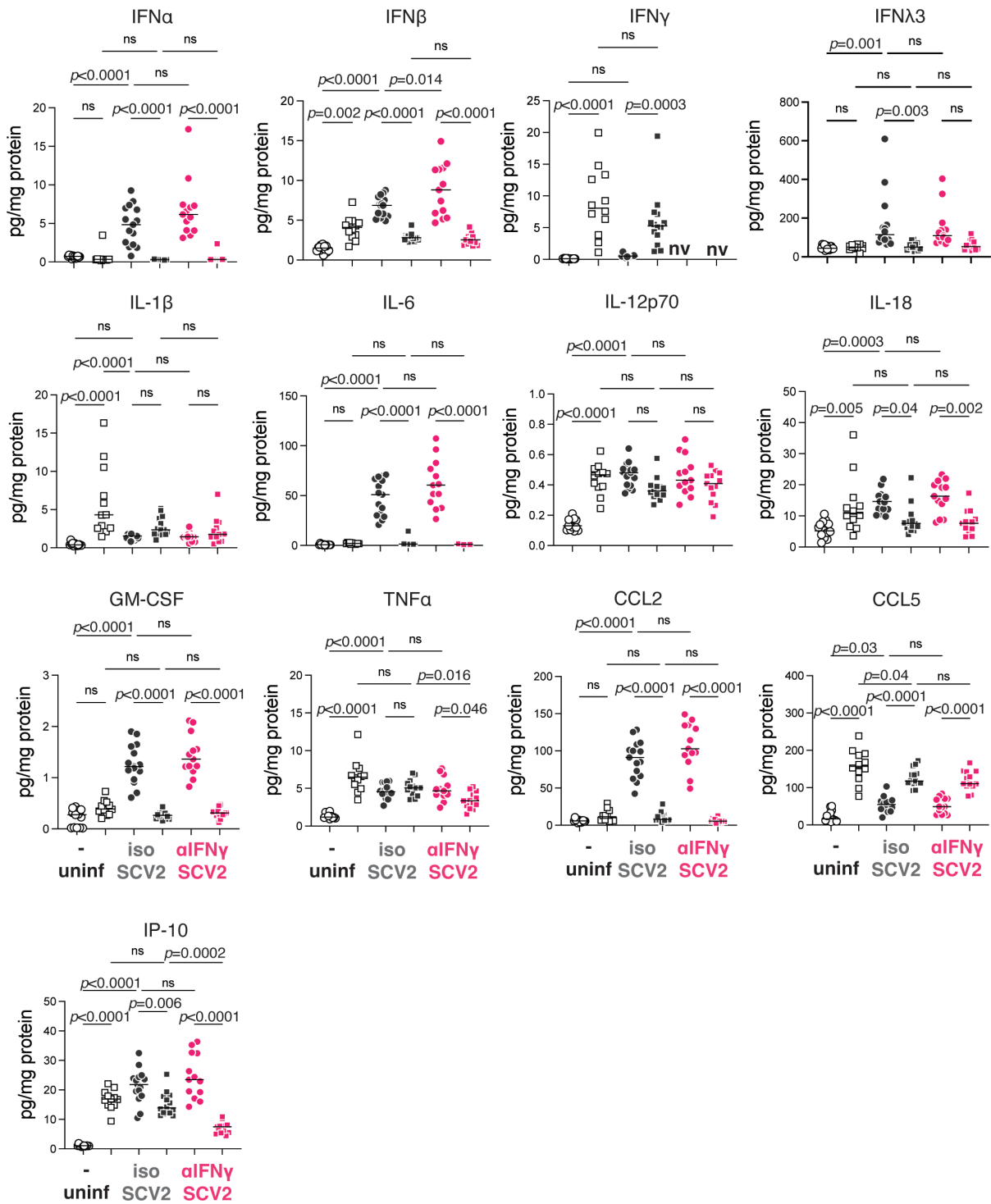


Figure S3: BCG suppresses SARS-CoV-2-induced inflammatory cytokines independent of IFN γ .

B6 mice were inoculated with BCG or PBS *iv* 40-45 days prior to intranasal challenge with SARS-CoV-2 (SCV2) B.1.351. Infected animals received an IFN γ neutralizing antibody or isotype control 1 day prior to and 1 day following SARS-CoV-2 instillation. Lungs were harvested 3 days after viral challenge. Cytokines were measured by multiplex assay or ELISA and normalized to total protein content (PBS $n=13$, BCG $n=12$, PBS+SCV2+iso $n=15$, BCG+SCV2+iso $n=14$, PBS+SCV2+aIFN γ $n=13$, BCG+SCV2+aIFN γ $n=13$; pooled from 3

independent experiments; One-Way ANOVA with Tukey post-test). Not significant (ns) $p > 0.05$; * $p < 0.05$; **, $p < 0.01$; *** $p < 0.001$; **** $p < 0.0001$. nv = not valid due to administration of anti-IFN γ antibody. Source data are provided as a Source Data file.

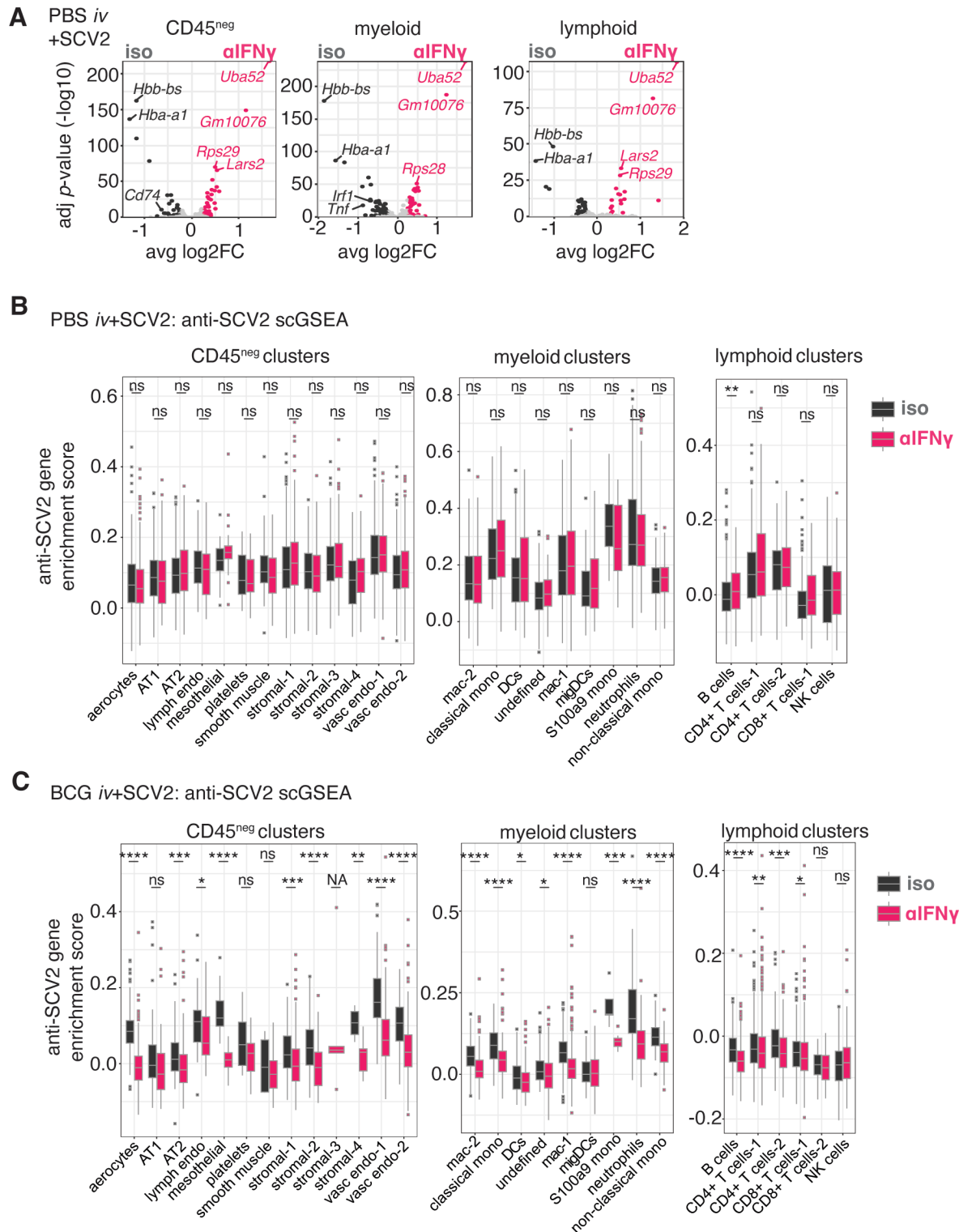


Figure S4: IFN γ neutralization reduces enrichment of genes associated with SARS-CoV-2 restriction in mice previously inoculated with BCG *iv*.

B6 mice were inoculated with PBS or BCG *iv* 40-45 days prior to intranasal challenge with SARS-CoV-2 (SCV2) B.1.351. Infected animals received an IFN γ neutralizing antibody or isotype control 1 day prior to and 1 day following SARS-CoV-2 instillation. Lungs were harvested 3 days after viral challenge. **(A)** Volcano plots show DEGs between isotype and anti-IFN γ treated mice inoculated *iv* with PBS prior to SARS-CoV-2 challenge across CD45^{neg}, myeloid and lymphoid lineages that were manually annotated from the Seurat clustering

shown in Fig1C and FigS1A. DEGs are shown in dark gray or pink and were defined as $\log_2FC > 0.25$ and $p < 0.05$ (Wilcoxon Rank Sum test with Bonferroni correction). Light grey points denote genes that did not reach statistical significance. Gene lists and their associated FC and p -values can be found in Supplementary Data 8-10. **(B-C)** scGSEA was performed on Seurat defined clusters (Fig1C and FigS1A) for each experimental condition using a manually curated “anti-SARS-CoV-2” gene set (Supplementary Data 11). Box plots show “anti-SARS-CoV-2” gene set enrichment scores for individual clusters comparing isotype and anti-IFN γ treatment groups for PBS+SCV2 control mice **(B)** and animals inoculated with BCG *iv* prior to SARS-CoV-2 challenge (BCG *iv*+SCV2) **(C)**. Statistical significance was assessed by Wilcoxon Rank Sum test with Bonferroni correction. Not significant (ns) $p > 0.05$; * $p < 0.05$; **, $p < 0.01$; *** $p < 0.001$; **** $p < 0.0001$. Exact p -values are reported in the Source Data file. Data are shown as median, quartiles \pm range. Source data are provided as a Source Data file.

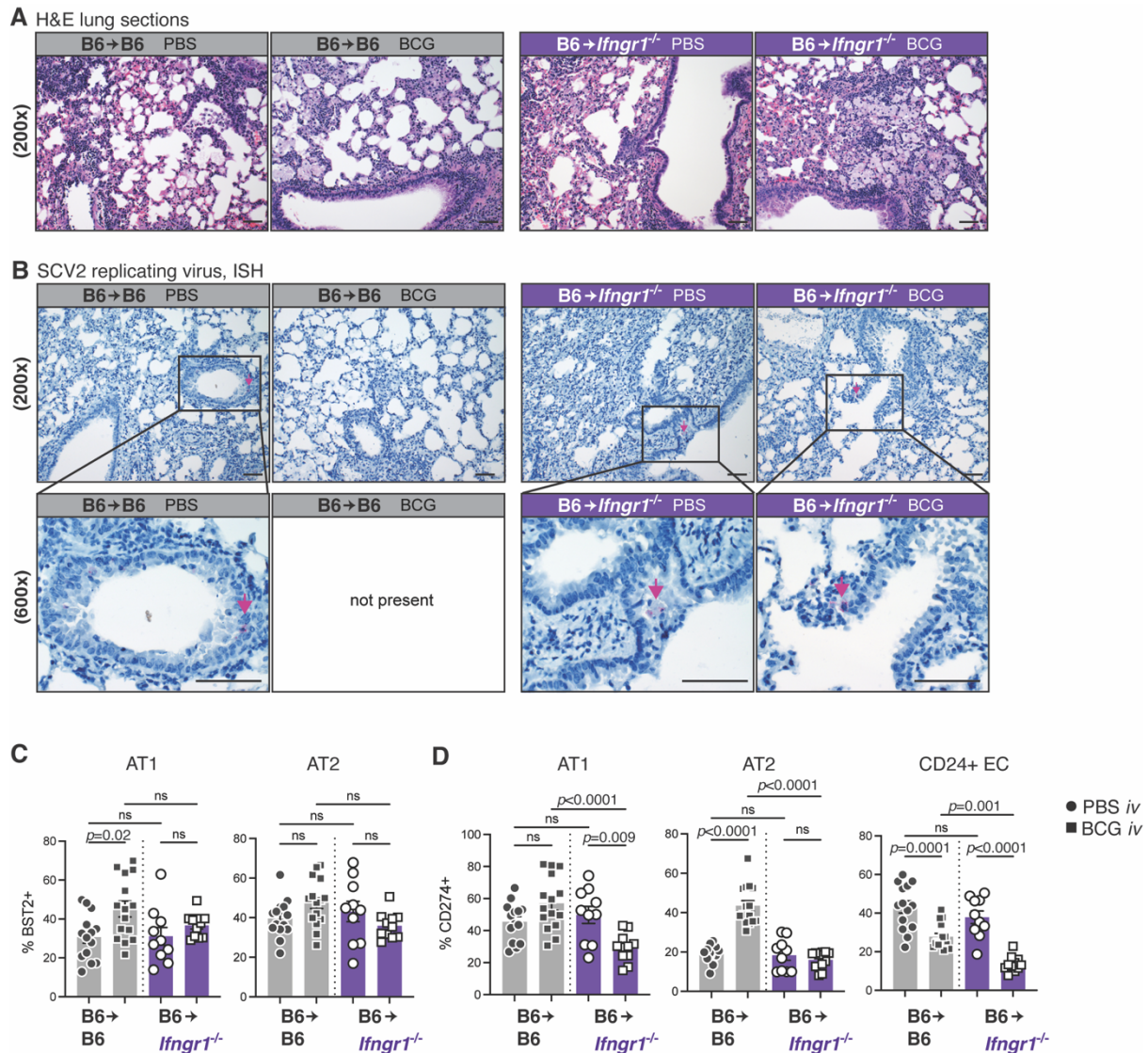


Figure S5: Absence of IFN γ R1 signaling in the non-hematopoietic compartment increases viral replication and reduces CD274 expression in epithelial cells of mice previously *iv* inoculated with BCG.

B6 or *Ifngr1*^{-/-} CD45.2⁺ mice were irradiated and reconstituted with B6 congenic CD45.1⁺ bone marrow. Chimeras were inoculated with BCG or PBS *iv* 40-45 days prior to intranasal challenge with SARS-CoV-2 (SCV2) B.1.351. Lungs were harvested 3 days after viral challenge. **(A)** Representative images of H&E-stained lung sections (B6 PBS *n*=9, B6 BCG *n*=10, *Ifngr1*^{-/-} PBS *n*=6, *Ifngr1*^{-/-} BCG *n*=8; 2 independent experiments). Scale bar=50 μ m. **(B)** Example images of *in situ* hybridization of a probe targeting replicating SARS-CoV-2 (B6 PBS *n*=9, B6 BCG *n*=10, *Ifngr1*^{-/-} PBS *n*=6, *Ifngr1*^{-/-} BCG *n*=8; 2 independent experiments). Scale bar=50 μ m. **(C)** Expression of BST2 by AT1 and AT2 cells as determined by flow cytometry. **(D)** Expression of CD274 by AT1, AT2 and CD24⁺ epithelial cells as determined by flow cytometry. The epithelial cell gating strategy is shown in FigS6A. B6 PBS *n*=14, B6 BCG *n*=15, *Ifngr1*^{-/-} PBS *n*=10, *Ifngr1*^{-/-} BCG *n*=11; pooled from 3 independent experiments; One-Way ANOVA with Tukey post-test. Not significant (ns) *p*>0.05. Source data are provided as a Source Data file.

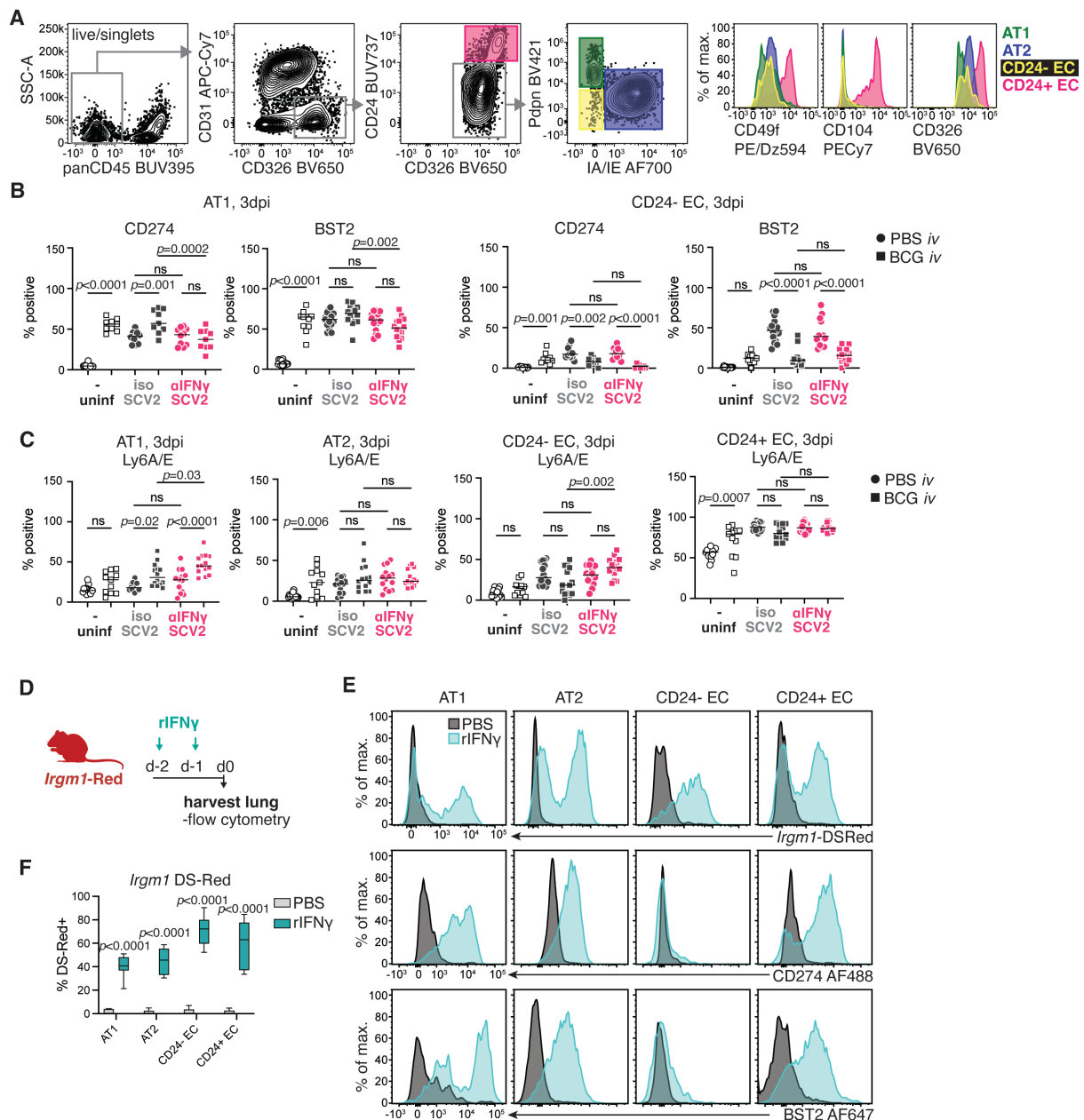


Figure S6: IFN γ induces expression of anti-viral markers in pneumocytes and CD24+ epithelial cells.

(A) Gating strategy employed to identify pulmonary epithelial cell subsets. (B-C) B6 mice were inoculated with BCG or PBS *iv* 40-45 days prior to intranasal challenge with SARS-CoV-2 (SCV2) B.1.351. Infected animals received an IFN γ neutralizing antibody or isotype control AT1 1 day prior to and 1 day following SARS-CoV-2 instillation. Lungs were harvested 3 days after viral challenge and the indicated epithelial cell types assessed for CD274 ($n=10$ /PBS group, $n=9$ /BCG group; pooled from 2 independent experiments; One-Way ANOVA with Tukey post-test), BST2 and Ly6A/E (PBS $n=15$, BCG $n=12$, PBS+SCV2+iso $n=15$, BCG+SCV2+iso $n=14$, PBS+SCV2+aIFN γ $n=14$, BCG+SCV2+aIFN γ $n=14$; pooled from 3 independent experiments; One-Way ANOVA with Tukey post-test) expression by flow cytometry. Not significant (ns) $p > 0.05$. (D-F) *Irgm1-Red* (M1-Red) mice were treated with PBS or rIFN γ intranasally on 2 consecutive days. Lungs were harvested 1 day after the last treatment. (D) Schematic of experimental protocol. (E) Representative expression profiles of *Irgm1* DS-Red, BST2 AF647 and CD274 AF488 across different epithelial subsets. (F) Expression of the *Irgm1* DS-Red

reporter across different epithelial cell types (PBS $n=5$, rIFN γ $n=8$; pooled from 2 independent experiments, two-tailed unpaired t-test). Source data are provided as a Source Data file.

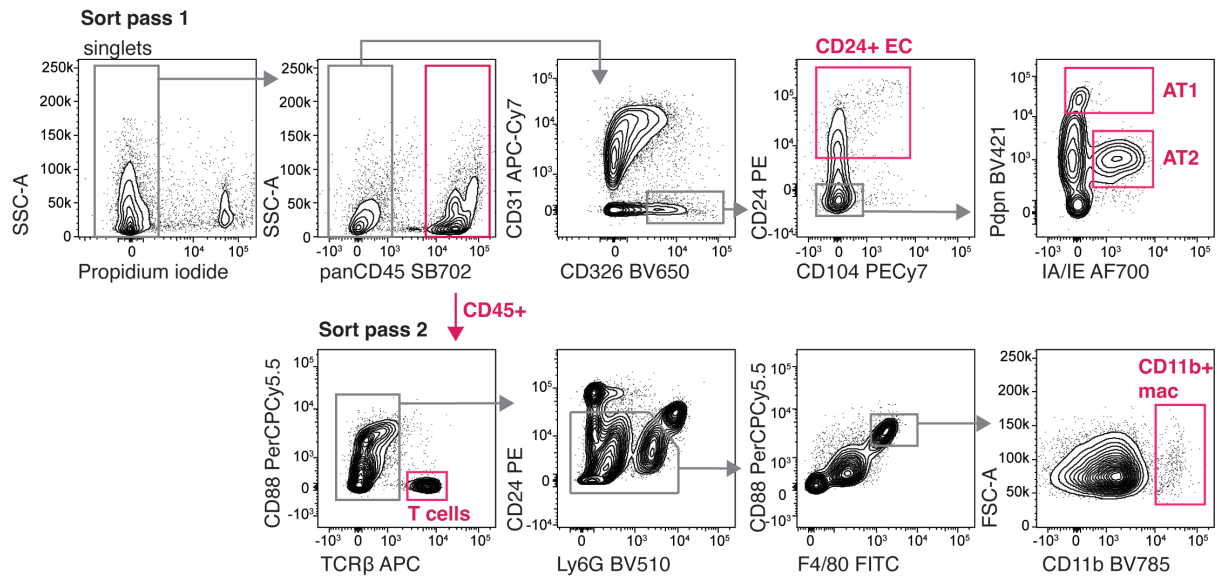


Figure S7: Cell sort gating strategy.

Gating strategy employed to sort pulmonary epithelial cell subsets, T cells and CD11b+ macrophages from lung tissue of SARS-CoV-2 infected K18-hACE2 mice.